arXiv:hep-ph/9910231v3 12 Nov 1999

CERN-TH/99-269
IFT-99/22
hep-ph/9910231

FIXED POINTS IN THE EVOLUTION OF NEUTRINO MIXINGS

Piotr H. Chankowski[a,b)], Wojciech Królikowski[b)] and Stefan Pokorski[b)]

ABSTRACT

We derive the renormalization group equations for the neutrino masses and mixing angles in explicit form and discuss the possible classes of their solutions. We identify fixed points in the equations for mixing angles, which can be reached during the evolution for several mass patterns and give $\sin^2 2\theta_{sol} = \sin^2 2\theta_{atm} \sin^2\theta_3/(\sin^2\theta_{atm}\cos^2\theta_3 + \sin^2\theta_3)^2$, consistently with the present experimental information. Further experimental test of this relation is of crucial interest. Moreover, we discuss the stability of quantum corrections to neutrino mass squared differences. Several interesting mass patterns show stability in the presence of fixed point solutions for the angles.

[a)] Theory Division, CERN, Geneva, Switzerland
[b)] Institute of Theoretical Physics, Warsaw University, Poland

CERN-TH/99-269
IFT-99/22
October 1999

1 Introduction

Observation of atmospheric [1] and solar [2] neutrinos provide important indications that neutrinos oscillate between different mass eigenstates. Interpreting each observation in terms of two-flavour mixing the oscillations of atmospheric neutrinos require $\Delta m^2_{atm} \sim 2 \times 10^{-3}$ eV^2 and a nearly maximal mixing angle $\sin^2 2\theta_{atm} \geq 0.82$. For solar neutrinos, several solutions of their deficit problem are possible. The vacuum oscillation (VO) solution requires $\Delta m^2_{sol} \sim 10^{-10}$ eV^2 and $\sin^2 2\theta_{sol} \geq 0.67$, whereas the the so-called MSW solution requires $\Delta m^2_{sol} \sim \mathcal{O}(10^{-5})$ eV^2 and $\sin^2 2\theta_{sol} \geq 0.5$ (large mixing angle solution - LAMSW) or $4 \times 10^{-3} \lesssim \sin^2 2\theta_{sol} \lesssim 1.3 \times 10^{-2}$ (small mixing angle solution - SAMSW). Combining these results with non-observation of the dissappearance of $\bar{\nu}_e$ in the reactor experiments (in particular in CHOOZ [3]) sensitive to $\Delta m^2 \gtrsim 10^{-3}$ eV^2 and $\sin^2 2\theta \gtrsim 0.2$, the atmospheric and solar neutrino oscillations can be explained in terms of three known flavours of neutrinos[1], the assumption which we adopt in this paper, as $\nu_\mu \to \nu_\tau$ and $\nu_e \to \nu_x$ oscillations with $\nu_x = \nu_\mu$ if the mixing was two flavour one.

With accumulating data, considerable attention has been focused on the determination of the full Maki-Nakagawa-Sakata (MNS) 3×3 unitary mixing matrix [6] which is conveniently parametrized by 3 angles (we set the phase $\delta = 0$)

$$U = \begin{pmatrix} c_1 c_3 & s_1 c_3 & s_3 \\ -s_1 c_2 - c_1 s_2 s_3 & c_1 c_2 - s_1 s_2 s_3 & s_2 c_3 \\ s_1 s_2 - c_1 c_2 s_3 & -c_1 s_2 - s_1 c_2 s_3 & c_2 c_3 \end{pmatrix} \tag{1}$$

where s_i and c_i denote $\sin\theta_i$ and $\cos\theta_i$, respectively.

Defining $\Delta m^2 \equiv m_2^2 - m_1^2$ with $|\Delta m^2| = \Delta m^2_{sol}$ and $\Delta M^2 \equiv m_3^2 - m_2^2$ with $|\Delta M^2| = \Delta m^2_{atm}$, the CHOOZ experiment measures (with $\Delta M^2 \gg \Delta m^2$ and $\sin^2(\Delta m^2 L/4E) \approx 0$)

$$P(\bar{\nu}_e \to \bar{\nu}_e) = 1 - 4U_{13}^2(1 - U_{13}^2) \sin^2\left(\frac{\Delta M^2 L}{4E}\right) \tag{2}$$

and the negative result of the search constraints $s_3 = U_{13}$: $s_3^2 \lesssim 0.2$.

For the solar neutrino oscillations we have (averaging $\sin^2(\Delta M^2 L/4E)$ to 1/2):

$$P_{3\times3}(\nu_e \to \nu_e) = c_3^4 P_{2\times2}(\nu_e \to \nu_e) + s_3^4 \tag{3}$$

(for this formula to account also for the MSW solution one has to mutiply the electron density in the Sun in the 2-flavour probability $P_{2\times2}$ by c_3^2 [7]). In the limit $s_3 = 0$, $\theta_{sol} = \theta_1$. However, since in general $U_{31} \neq 0$, $P(\nu_e \to \nu_\tau) \neq 0$.

For the atmospheric neutrinos

$$P(\nu_\mu \to \nu_\tau) = 4(U_{23}U_{33})^2 \sin^2\left(\frac{\Delta M^2 L}{4E}\right) = 4s_2^2 c_2^2 c_3^2 \sin^2\left(\frac{\Delta M^2 L}{4E}\right) \tag{4}$$

---

[1] We leave out the not yet confirmed LSND result [4]. All three measurements can be explained only if there exists sterile neutrinos, e.g. light right-handed ones [5].

so, in the limit $s_3 = 0$, $\theta_{atm} = \theta_2$.

Thus, up to some uncertainties in $|U_{13}| = |s_3|$, for each mentioned earlier solution to the atmospheric and solar neutrino problems we can infer the *gross* pattern of the 3×3 mixing matrix. The striking features are large mixing angles θ_2 and, for VO and LAMSW solutions, θ_1. Measuring s_3 is very important, as the dependence of the fitted s_1 and s_2 on s_3 is not totally negligible [8, 9, 10].

Large number of papers addressed the issue of theoretical explanation of neutrino masses and mixings and of incorporating it into some global solution to the flavour problem [11, 12, 13, 14, 15, 16, 17, 18, 19, 20, 21, 22]. One attractive possibility for giving the three flavours of neutrinos small Majorana masses is the seesaw mechanism which generates in the effective low energy theory (MSSM or the SM) a dimension five operator. In the two-component notation it reads:

$$\mathcal{L}_{dim\ 5} = -\frac{1}{4M}\mathcal{C}^{ab}(Hl^a)(Hl^b) + h.c. \tag{5}$$

where a is generation index, l is the ordinary lepton $SU(2)$ doublet, H is the hypercharge $+1/2$ Higgs doublet (i.e. $H^{(2)}$ in the MSSM) and the matrix $\mathcal{C}$ is dimensionless because we have factorized out the overall scale M of the heavy, right-handed neutrino mass matrix. This operator, after the electroweak symmetry breaking, is the origin of the left-handed neutrino Majorana mass term

$$\mathcal{L}_{\nu\ mass} = -\frac{1}{2}m_\nu^{ab}\nu^a\nu^b + h.c. \tag{6}$$

with $m_\nu = (v^2/4M)\mathcal{C}$ where $v/\sqrt{2} = \langle H_2 \rangle$. After the unitary rotation $\nu^a \rightarrow V_L^{ab}\nu^b$ diagonalizing the neutrino[2] mass matrix $\mathcal{C}$

$$V_L^T \mathcal{C} V_L = C_D \equiv \mathrm{diag}(C_1, C_2, C_3) \sim \mathrm{diag}(m_1, m_2, m_3) \tag{7}$$

the charged current weak neutrino interactions depend on the MNS unitary matrix (1), $U = E_L^\dagger V_L$ and the rotations E_L are defined by

$$E_L^\dagger \mathcal{M}_e^2 E_L = H_e^2 \equiv \mathrm{diag}(h_e^2, h_\mu^2, h_\tau^2) \tag{8}$$

($\mathcal{M}_e^2 \equiv Y_e^\dagger Y_e$ is the square of the lepton Yukawa coupling matrix and h_a^2 are its eigenvalues). It is this matrix whose elements are probed in the neutrino oscillation experiments. In the effective theory below the scale M, with the right-handed neutrinos decoupled we can work in the charged lepton mass eigenstate basis, fixed by the diagonalization of the charged lepton Yukawa matrix at the scale M and then $U = V_L$.

The measured neutrino mass matrix $m_\nu = (v^2/M)UC_DU^T$ is linked to the fundamental mass generation mechanism by two steps. The first one (in the top-down approach) is the renormalization group (RG) evolution of the neutrino and charged lepton Yukawa coupling matrices Y_ν and Y_e, respectively, from the scale at which they are fixed by some theory of flavour (presumably at the GUT scale) down to the right-handed Majorana mass scale $M < M_{GUT}$. At that scale the right-handed neutrinos with the Majorana mass matrix $\hat{M}$ are integrated out and one obtains the Standard Model (SM) or its supersymmetric extension (MSSM) with the Majorana mass matrix of the light neutrinos given by the operator (5). The effective neutrino Majorana mass matrix $\mathcal{C}(M)$ at the scale M is dependent on both, neutrino and charged lepton original Yukawa textures at M_{GUT} and on $\hat{M}$.

---

[2] We will always assume that m_3 is positive and allow for negative signs of m_1 and/or m_2.

The second step consists of the renormalization group evolution of this operator down to the electroweak scale M_Z, which provides unambiguous mapping of the pattern at the scale M into the measured pattern at M_Z scale. Once we choose to work with the SM or the MSSM the physics below the scale M is almost unambiguous[3] and it is interesting to study the effects of quantum corrections to the neutrino mass matrix $\mathcal{C}(M)$ summarized in its renormalization group (RG) evolution down to M_Z. We find it convenient to work directly with m_a's and U_{ab}'s [4] rather than with elements of the matrix m_ν since, as we shall see, the evolution of mass eigenstates and mixing angles often allows for easy qualitative discussion.

In the present paper we extend earlier discussions [24, 25, 26] by, first, writting down the renormalization group equations for the neutrino mass eigenvalues and mixing angles between the three flavours of neutrinos, in the MSSM (and the SM). We point out the main differences between the evolution with 3×3 mixing or 2×2 mixing. Next, we discuss in some detail the solutions to the RGE's for mixing angles and their dependence on the mass eigenvalue patterns: $m_3^2 \approx \Delta M^2 \gg m_2^2, m_1^2$ (hierarchical), $m_1^2 \approx m_2^2 \approx \Delta M^2 \gg m_3^2$ (inversely hierarchical) and $m_1^2 \approx m_2^2 \approx m_3^2 \sim \mathcal{O}(\Delta M^2)$ or larger (degenerate), which are consistent with the measured mass squared differences. We identify several infrared (IR) fixed points in the RG equations for mixing angles, which can be reached for some range of neutrino masses and are compatible with the present experimental information on the mixing angles.

Finally, we discuss the stability with respect to quantum corrections of the three neutrino mass eigenvalue patterns which turns out to be correlated with the character of the evolution of the angles. In our formalism, we can reproduce in a very simple way the earlier results [24, 25, 26], in particular, those on the possibility of the VO solution with the stability of the inversely hierarchical or degenerate patterns.

2 RGE for neutrino masses and mixing angles

The importance of the scale dependence of the coefficient $\mathcal{C}$ of the operator (5) have been first emphasized in ref. [27, 28]. The derived there renormalization group equation in the MSSM reads[5]

---

[3] In the of the SM there is a slight dependence of the overall scale of the neutrino masses on the Higgs boson quartic coupling λ (i.e. on the Higgs boson mass) and in the MSSM on the assumed scale of supersymmetry breaking which we will ignore in the discussion which follows.

[4] For similar approach in the quark sector see [23].

$$\frac{d}{dt}\mathcal{C} = -K\mathcal{C} - \mathcal{C}\mathcal{M}_e^2 - (\mathcal{M}_e^2)^T\mathcal{C} \tag{9}$$

with $\mathcal{M}_e^2 = H_e^2$ (diagonal) in the basis we are working and where

$$K \equiv \left[-\frac{6}{5}g_1^2 - 6g_2^2 + 6\mathrm{Tr}\mathcal{M}_u^2\right], \tag{10}$$

$\mathcal{M}_u^2 \equiv Y_u^\dagger Y_u$ is the square of the up-type quarks Yukawa coupling matrix, $g_1^2 \equiv (5/3)g_y^2$, $t = (1/16\pi^2)\log(M/Q)$ and M is the large Majorana scale. In the SM the correct form of the equation was given in ref. [30] and has the same form with $-(6/5)g_1^2 \rightarrow +2\lambda$ (λ is the scalar quartic coupling), $-6g_2^2 \rightarrow -3g_2^2$, $6\mathrm{Tr}\mathcal{M}_u^2 \rightarrow \mathrm{Tr}(6\mathcal{M}_u^2 + 6\mathcal{M}_d^2 + 2\mathcal{M}_e^2)$ and the coefficients of the last two terms are $+1/2$ (instead of -1).

Equation (9) can be elegantly solved [31], since in the absence of right-handed neutrinos below the scale M the matrix E_L defined in (8) does not run. Thus, in the basis in which the leptonic Yukawa matrix is diagonal the equation (9) has the obvious solution

$$\mathcal{C}(t) = I_K\mathcal{I}\mathcal{C}(0)\mathcal{I} \tag{11}$$

where $\mathcal{I} = \mathrm{diag}(I_e, I_\mu, I_\tau)$, and

$$I_K \equiv \exp\left(-\int_0^t K(t')dt'\right), \qquad I_a \equiv \exp\left(-\int_0^t h_a^2(t')dt'\right). \tag{12}$$

The only role of the factor I_K is to change the overall scale of the neutrino masses during the evolution. For $M = 10^{10-15}$ GeV, $I_K \approx 0.9 - 0.6$ with smaller values for lower $\tan\beta$ due to the enhancement of the top quark Yukawa coupling in K.

Although the solution to the RG equation for the matrix $\mathcal{C}$ is simple, qualitative features of the running of the mass egenvalues m_a and the MNS mixing matrix U are often masked by the diagonalization procedure. In this paper we derive the RGE directly for m_a and U.

Following the method of ref. [32], the RG equation for the matrix $V_L = U$ (in the charged lepton mass eigenstate basis) can be written as

$$\frac{d}{dt}U = -U\varepsilon_\nu \quad \text{with} \quad \varepsilon_\nu^\dagger = -\varepsilon_\nu \tag{13}$$

where the matrix ε_ν is antihermitean, to preserve unitarity of U. It is determined by the requirement that the matrix $\mathcal{C}(t)$ is diagonalized by $U(t)$ at any scale and the RHS of

$$\frac{d}{dt}(U^T\mathcal{C}U) = \frac{d}{dt}C_D = -\varepsilon_\nu^T C_D - C_D\varepsilon_\nu - KC_D - C_D U^\dagger H_e^2 U - U^T H_e^2 U^\star C_D \tag{14}$$

---

[5] The MSSM RGEs given in ref. [28] allow to treat also the case in which squarks and/or gluino are much heavier than sleptons, charginos and neutralinos so that the decoupling procedure [29] can be employed; in this case there are four different (in component fields) operators which mix below the squark/gluino treshold. Above it one has (in the notation of ref. [28]) $c_1^{ab} = 2c_{12}^{ab} = 2c_{21}^{ab} = c_3^{ab} \equiv \mathcal{C}^{ab}$ and the four equations of ref. [28] merge into the one quoted here (derived independently also in ref. [30]).

is diagonal. For real matrices $\mathcal{C}$ and $\mathcal{M}_e^2$ which we consider here, the MNS matrix U is real and orthogonal and ε_ν is antisymmetric. We get therefore

$$\varepsilon_\nu^{ab} \;=\; -\frac{C_a + C_b}{C_a - C_b}(U^T H_e^2 U)_{ab} \qquad \text{for } a \neq b, \qquad \varepsilon_\nu^{aa} = 0. \tag{15}$$

The running of the eigenvalues is then given by

$$\frac{d}{dt}C_a = -\sum_{b=e,\mu\tau}(K + 2h_b^2 U_{ba}^2)C_a, \quad a = 1,2,3 \tag{16}$$

and the running of elements of the MNS matrix is given by

$$\frac{d}{dt}U_{ab} = \sum_{d\neq b}\frac{C_d + C_b}{C_d - C_b}U_{ad}(U^T H_e^2 U)_{db}. \tag{17}$$

If two of the three eigenvalues, say C_a and C_b, are equal at some scale t there is the obvious freedom in choosing the matrix $U(t)$, corresponding to the redefinition $U(t) \to \tilde{U}(t) = U(t)R$ where R is a rotation in the ab plane. This freedom is eliminated by quantum corrections, since for the evolution, R has to be fixed by the condition

$$(\tilde{U}^T H_e^2 \tilde{U})_{ab}(t) = (\tilde{U}^T H_e^2 \tilde{U})_{ba}(t) = 0 \tag{18}$$

so that equation (17) in nonsingular.

Eqs. (16,17) give directly the running of the the measurable parameters. It is straighforward to derive the equations for the three independent parameters s_1, s_2 and s_3. Neglecting h_e and h_μ Yukawa couplings we get:

$$\begin{aligned} \dot{s}_1 &= -c_1(s_1 s_2 - c_1 c_2 s_3)(-c_1 s_2 - s_1 c_2 s_3)A_{21}h_\tau^2 \\ &- s_1 c_1 c_2 s_3(s_1 s_2 - c_1 c_2 s_3)A_{31}h_\tau^2 + c_1^2 c_2 s_3(-c_1 s_2 - s_1 c_2 s_3)A_{32}h_\tau^2 \end{aligned} \tag{19}$$

$$\dot{s}_2 \;=\; s_1 c_2^2(s_1 s_2 - c_1 c_2 s_3)A_{31}h_\tau^2 - c_1 c_2^2(-c_1 s_2 - s_1 c_2 s_3)A_{32}h_\tau^2 \tag{20}$$

$$\dot{s}_3 \;=\; -c_1 c_2 c_3^2(s_1 s_2 - c_1 c_2 s_3)A_{31}h_\tau^2 - s_1 c_2 c_3^2(-c_1 s_2 - s_1 c_2 s_3)A_{32}h_\tau^2 \tag{21}$$

where $A_{ab} \equiv (C_a + C_b)/(C_a - C_b) = (m_a + m_b)/(m_a - m_b)$.

Eqs. (16-21) give us several immediate results. Neglecting the electron and muon Yukawa couplings, the solutions for squared mass eigenvalues read:

$$m_a^2(t) = m_a^2(0) I_K^2 \exp\left(-\int_0^t 4h_\tau^2(t')U_{3a}^2(t')dt'\right) \tag{22}$$

Observe that, since $I_K^2 < 1$, the masses always decrease top-down. We also see that the possibility of some change caused by the evolution in mass pattern resides solely in the differences in the mixing matrix elements U_{3a} and their RG running. With $h_\tau^2 \approx (\tan\beta/100)^2$, $t \approx 0.12$ for

$M = 10^{10}$ GeV and U_{3a}^2 typically varying between 0 and 1/4 (except for U_{33}^2) the exponent is at most of order of $\epsilon \equiv h_\tau^2 \log(M/M_Z)/16\pi^2 \approx \tan^2\beta \times 10^{-5} < 2.5 \times 10^{-2}$ for $\tan\beta < 50$. We can then estimate the changes in the mass squared differences:

$$\Delta m_{ab}^2(t) \equiv m_a^2(t) - m_b^2(t) = \Delta m_{ab}^2(0) - (\eta_a m_a^2(0) - \eta_b m_b^2(0))\epsilon \tag{23}$$

where we have neglected I_K which is always close to 1 and the factors $\eta_{a(b)} > 0$ are typically in the range $0-2$, depending on the values of U_{3a} factors and their evolution. Taking (for definiteness) $\Delta m_{ab}^2(0) = 0$, we see that the evolution of $\Delta m_{ab}^2(t)$ is limited by $m_a^2(0)\epsilon$ or $m_b^2(0)\epsilon$, i.e. by the value of the larger mass.

A spectacular feature of eq. (17) or eqs. (19-21) is the existence of fixed points at $U_{ab} = 0$. The character of the fixed points (UV or IR) and the rate of approaching them depend on the mass factors A_{ab}. This point will be discussed in detail later on. We note the possibility of a large factor A_{ab}, for nearly degenerate and of the same sign eigenvalues m_a and m_b, which can permit a rapid approach to fixed points and drastically change the pattern of mixing at M_Z during the evolution from M. [6] In the solutions (11) for the matrix $\mathcal{C}$ this point is encoded in the diagonalization procedure one has to perform *after* the running. The equivalence of the two approaches can be proven by diagonalizing the matrix $\mathcal{C}(t+\Delta t)$ using the ordinary perturbation calculus. In the first order in Δt one obtains then precisely eq. (17). This approach also can serve to justify eq. (18).

Finally we comment on two flavour mixing (which is sometimes good approximation to the more complex three flavour mixing). The 2×2 MNS matrix is an ordinary orthogonal rotation matrix. The general formalism applied to the mixing between say, second and third generation, gives

$$\frac{d}{dt}\sin\vartheta = \sin\vartheta\cos^2\vartheta\frac{C_3 + C_2}{C_3 - C_2}(h_3^2 - h_2^2). \tag{24}$$

It is then straighforward to write down the equation for the evolution of $\sin^2 2\vartheta$:

$$\frac{d}{dt}\sin^2 2\vartheta = 2\sin^2 2\vartheta\cos 2\vartheta\frac{C_3 + C_2}{C_3 - C_2}(h_3^2 - h_2^2). \tag{25}$$

Observe also that eq. (25), contrary to the original one (24), cannot be used for the initial condition $\cos 2\vartheta = 0$. This is because $\cos 2\vartheta = 0$ is the point at which the uniqueness of the solution of the differential equation (25) is violated. It has there two solutions: a t-dependent one which is the solution also to eq. (24) and the second one, $\sin^2 2\vartheta \equiv 1$, which does not solve eq. (24). Thus, the previous claims that the maximal mixing $\sin^2 2\theta = 1$ is stable against the RG running are not correct [30, 33, 34, 21, 35]. It is easy to see that, for the two-flavour evolution to be good approximation to the full three-flavour evolution of θ_2 as given by eq. (20), two conditions must be met: i) θ_3 has to be small and ii) the factors A_{31} and A_{32} have to be comparable.

---

[6] The possibility of strong changes in the mixing pattern due to the evolution has been pointed out earlier for 2×2 mixing [30].

3 Evolution of mixing angles

The equations derived in the previous section can be used for a systematic analysis of the RG evolution of the mass and mixing patterns which are consistent with neutrino experimental data. To fix the framework we universally impose the following constraints at the electroweak scale: $\Delta M^2 = 10^{-3}$ eV^2, $\sin^2 2\theta_2 > 0.82$ and $\sin^2\theta_3 \equiv s_3^2 < 0.2$. Furthemore, for each solution - VO, LAMSW and SAMSW - to the solar neutrino deficit problem we assume the corresponding value of $\sin^2 2\theta_1$ and consider all mass configurations that are consistent with the respective Δm^2. The list of acceptable low energy mass patterns is, therefore, as follows:

I $\Delta M^2 \approx m_3^2 \gg m_1^2, m_2^2$ (hierarchical) with two distinct subpatterns:

  $\Delta m^2 \approx m_{2(1)}^2 \gg m_{1(2)}^2$ or

  $m_{2(1)}^2 \gtrsim m_{1(2)}^2$ with $m_{2(1)}^2$ ranging from $m_{2(1)}^2 \gtrsim \Delta m^2$ to $m_{2(1)}^2 \gg \Delta m^2$ (the latter being, strictly speaking, possible only in the VO case; for SAMSW and LAMSW solutions, with our representative numbers $\Delta m^2 = 5\times 10^{-6}$ and 5×10^{-5} eV^2, respectively, $m_{2(1)}^2 \gg \Delta m^2$ violates the inequality $\Delta M^2 \approx m_3^2 \gg m_1^2, m_2^2$ and one gets the pattern III below). It is also necessary to distinguish the cases $m_1 m_2 < 0$ and $m_1 m_2 > 0$ [25, 24, 36]

II $\Delta M^2 \approx m_2^2, m_1^2 \gg m_3^2$ (inversely hierarchical). Here, also, the evolution depends on the choice $m_1 m_2 < 0$ (with $\Delta m^2 > 0$ or < 0) or $m_1 m_2 > 0$ (with $\Delta m^2 > 0$ or < 0)

III $m_3^2 \approx m_2^2 \approx m_1^2$ and all of the order or larger than ΔM^2 (degenerate). Here the evolution depends on the relative magnitudes (four different orderings satisfy our general constraints) and relative signs of the masses (we choose $m_3 > 0$ and for each ordering there are four inequivalent sign combinations).

Since the evolution of angles is less dependent on the evolution of mass eigenvalues than the other way around, it is convenient to begin our discussion with the former. It can be classified into several universal types of behaviour, depending on the magnitude of the factors A_{ab} in eqs. (19-21). We note that, neglecting the effects of mass evolution, all possible mass configurations contained in patterns I−III give one of the following four structures:

a) $A_{31} \approx A_{32}$ and $|A_{31}| \approx |A_{21}| \approx 1$

b) $A_{31} \approx A_{32}$ and $|A_{21}| \gg |A_{31}|$, $|A_{21}| \gg 1$

c) $A_{32} \approx A_{21} \approx 0$, $|A_{31}| \gg 1$

d) $A_{31} \approx A_{21} \approx 0$, $|A_{32}| \gg 1$

For *a*) and *b*), since $A_{31} \approx A_{32}$, equations (19-21) reduce to:

$$\begin{aligned} \dot{s}_1 &= -c_1(s_1 s_2 - c_1 c_2 s_3)(-c_1 s_2 - s_1 c_2 s_3) A_{21} h_\tau^2 - c_1 s_2 c_2 s_3 A_{32} h_\tau^2, \\ \dot{s}_2 &= s_2 c_2^2 A_{32} h_\tau^2, \\ \dot{s}_3 &= c_2^2 s_3 c_3^2 A_{32} h_\tau^2. \end{aligned} \tag{26}$$

Thus, the evolution of the atmospheric mixing angle is as in the two-generation equations (24) or (25). The first two patterns, hierarchical and inversely hierarchical give the A_{ab} factors as in *a*) or *b*). In addition, since for patterns I and II $|A_{32}| \approx 1$, the evolution of both, s_2 and s_3 is very weak (note that $s_2 = 0$ and/or $s_3 = 0$ are fixed points). Denoting

$$\xi_\tau \equiv \exp\left(-\int_0^t 2A_{32}(t')h_\tau^2(t')dt'\right) \approx \exp\left(-2A_{32}(0)\epsilon\right) \tag{27}$$

the solution for $s_2^2(t)$ reads

$$s_2^2(t) = s_2^2(0) / \left[s_2^2(0) + c_2^2(0)\xi_\tau\right] \tag{28}$$

and yields

$$\begin{aligned} \sin^2 2\theta_2(t) &= \xi_\tau \sin^2 2\theta_2(0) / \left[s_2^2(0) + c_2^2(0)\xi_\tau\right]^2 \\ &\approx \sin^2 2\theta_2(0)\left[1 + 2\cos 2\theta_2(0) A_{32}(0)\epsilon\right] + \mathcal{O}(A_{32}^2\epsilon^2). \end{aligned} \tag{29}$$

The effect of the running for $\sin^2 2\theta_{atm}$ is a 2.5% change for extreme value of $\tan\beta \approx 50$. Since there is no large factor involved, the logarithmic approximation (the last line in eq. (29)) is very good. This is important for the evolution of the masses, discussed in the next section.

Moreover, we observe that, in the very good approximation of constant c_2, the solution for s_3 is also of the form (28), with $s_2(c_2) \to s_3(c_3)$ and $A_{32} \to c_2^2 A_{32}$ in the definition of ξ_τ.

For the solar mixing angle, in the approximation $s_3 = 0$, we have

$$\dot{s}_1 = s_1 c_1^2 s_2^2 A_{21} h_\tau^2 \tag{30}$$

and the solution for s_1 is of the form (28) too, with $s_2(c_2) \to s_1(c_1)$ and

$$\xi_\tau \to \xi'_\tau = \exp\left(-\int_0^t 2s_2^2(t')A_{21}(t')h_\tau^2(t')dt'\right). \tag{31}$$

With further specification to the structure *a*), occuring for $\Delta m^2 \approx m_{2(1)}^2 \gg m_{1(2)}^2$ and, in general, for $m_1 m_2 < 0$, the evolution of the angle s_1 is very weak, independently of the chosen solar solution. Since all $|A_{ab}| \lesssim 1$ the dependence on s_3 is weak (for $s_3^2 < 0.2$). We conclude that in case *a*) the evolution of all mixing angles is negligible and the existence of the fixed points at $U_{ab} = 0$ in eqs. (19-21) is irrelevant.

The evolution of s_1 is dramatically different for $|A_{21}\epsilon| \gg 1$, i.e. for $m_{2(1)}^2 > |\Delta m^2|$ and $m_1 m_2 > 0$. The presence of the fixed points becomes relevant but, since the evolution of s_2 and s_3 is still very weak ($|A_{32}| \approx 1$), they manifest themselves as two approximate fixed points

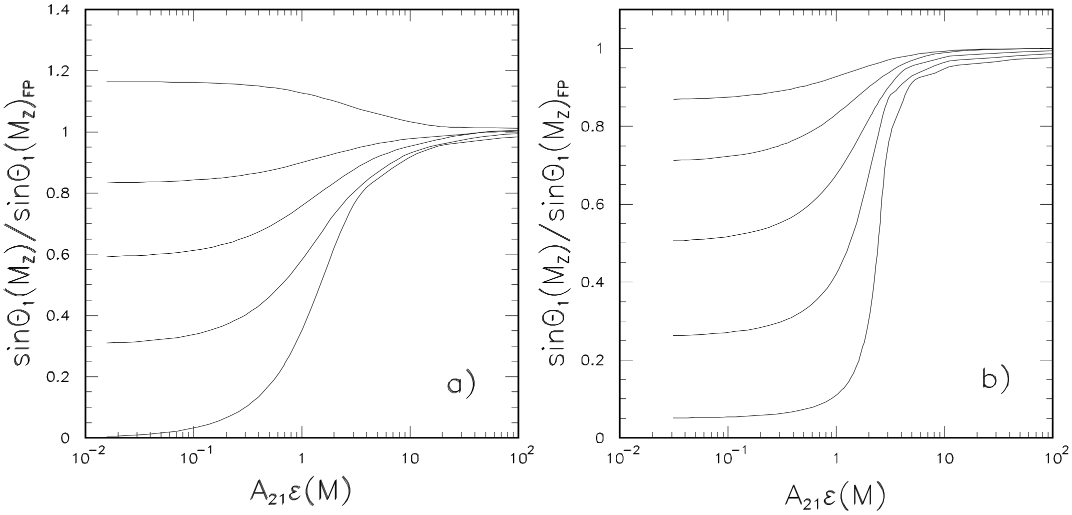

Figure 1: Approach to the IR fixed point for the angle θ_1 as a function of $A_{21}\epsilon(M)$ for two different values of s_3: a) $s_3^2 = 0.2$ and the hierarchy $|m_3| \gg |m_2| \gtrsim |m_1|$, b) $s_3^2 = (0.025)^2$ and the hierarchy $|m_2| \gtrsim |m_1| \gg |m_3|$. In both cases $m_1 m_2 > 0$ and we have taken $\sin^2 2\theta_2 = 0.9$ so that in case a) fixed point corresponds to $\sin^2 2\theta_1 = 0.8$ and in case b) to $\sin^2 2\theta_1 = 5 \times 10^{-3}$. Different lines correspond to different choices of $\theta_1(M)$ As explained in the text, for $|A_{21}|\epsilon \gg 1$ and $|A_{32}| \approx |A_{31}| \lesssim 1$, the evolution of θ_2 and θ_3 is negligible.

of the RG equations for s_1. One can easily check (for instance, by considering the equation for $d\tan\theta_1/dt = (1/c_1^3)\dot{s}_1$) that for $A_{21} > 0$ (i.e. for $\Delta m^2 > 0$) the point $U_{31} = 0$ is the UV fixed point and $U_{32} = 0$ is the IR fixed point. For $A_{21} < 0$ (i.e. for $\Delta m^2 < 0$) the situation is reversed. It is also interesting to notice that in the limit $s_3 = 0$ we can follow analytically the approach to the fixed points. In this limit the RG equation for s_1 has again the form (30) with the solution of the form (28) with the replacement (31). Therefore, for $A_{21} > 0$, in the top-down running the factor $\xi' \to 0$ exponentially with growing $A_{21}h_\tau^2 \log(M/M_Z)$ and, consequently, we obtain $s_1(t) = \pm 1$ (depending on its initial sign) and approach IR fixed point at $U_{32} = 0$. In the bottom-up evolution we approach $s_1^2(t) \approx 0$ exponentially, i.e. the UV fixed point at $U_{31} = 0$. For $A_{21} < 0$ we get the reversed situation, in accord with our general expectations.

Several comments are in order here. First, it is useful to remember the relation between $\sin^2 2\theta_1$ and $\sin^2 2\theta_2$ as the function of s_3 at $U_{31} = 0$ and $U_{32} = 0$ (i.e. for $\tan\theta_1 = s_3/\tan\theta_2$ and $\tan\theta_1 = -\tan\theta_2/s_3$, respectively). For both we get the following:

$$\sin^2 2\theta_1 = \frac{s_3^2 \sin^2 2\theta_2}{(s_2^2 c_3^2 + s_3^2)^2} \quad \text{with} \quad s_2^2 = \frac{1}{2}\left(1 \pm \sqrt{1 - \sin^2 2\theta_{atm}}\right). \tag{32}$$

Thus, both fixed points at IR are at present experimentally acceptable with the mixing close to bi-maximal for $s_3^2 \approx 0.2$ and with the SAMSW solution for $s_3 \approx 0$. This is interesting in the sense of the independence of initial conditions at the scale M.

Secondly, it is interesting to estimate the values of A_{21} and $\tan\beta$, for which the approach to the IR fixed points is seen. This is shown in Fig. 1. We can estimate that for approaching the fixed point during the evolution in the range (M_Z, M) one needs $A_{21}\epsilon(M) > 3$, i.e. for $\tan\beta = 20$ one needs $m_1 \approx m_2 \gtrsim 10^{-4}$ eV for the VO and $m_1 \approx m_2 \gtrsim 0.01$ eV for LAMSW or SAMSW solution.

Finally we note, that from the point of view of the initial conditions at the scale M, the UV fixed point looks not realistic as the neglected muon Yukawa coupling h_μ quickly destabilizes it during the evolution. We conclude that for hierarchical and inversely hierarchical mass patterns the evolution of the mixing angles is either very mild or shows (for $|A_{21}|\epsilon \gg 1$) fixed point behaviour. With higher precision experiments, it will be very interesting to confirm or disprove the IR fixed point relation between the angles.

The evolution of mixing angles in the degenerate case, $m_3^2 \approx m_2^2 \approx m_1^2 \sim \mathcal{O}(\Delta M^2)$ or larger, partly falls into the same classes of behaviour. Indeed, as long as $A_{31} \approx A_{32}$ and $|A_{21}| \gg |A_{31}|$, $|A_{21}| \gg 1$, the angles evolve according to the same equations (26). One can easily identify the eight mass patterns of the degenerate case that fall into this cathegory: the sufficient condition is that m_1 and m_2 are of the same sign. For the evolutions of s_1 we then closely follow the two possibilities (depending on the sign of A_{21}) discussed for the first two hierarchies with $m_1 m_2 > 0$. We simply note that larger values of $|A_{21}|$ are generic for the present case and, as seen in Fig. 1, the approach to the fixed points is faster. However, the evolution of s_2 and s_3 are mild only if m_1 and m_2 are negative ($A_{31} \approx A_{32} \approx 0$). For positive m_1 and m_2, we have $A_{31}\epsilon \approx A_{32}\epsilon$ and $|A_{32}\epsilon|$ can be much larger than 1 (depending on the overall mass scale 0.1 eV $\lesssim m_1 \lesssim$ 2 eV) so that the evolution of s_2 and s_3 is no longer negligible. According to the solution (28), s_2 is exponentially focused to $s_2(t) = 0$ or $s_2(t) = \pm 1$, depending on the sign of A_{32}, and on the direction of the evolution but independently of the values of s_1 and s_3. We stress again that $s_2(0) = \pm 1/\sqrt{2}$ i.e. $\sin^2 2\theta_{atm} = 1$ is not stable. The angle s_3 behaves in a similar way. Both angles can approach the value for which $\sin^2 2\theta_i = 0$ $(i = 2, 3)$, corresponding to the fixed points of their respective equations. This is experimentally acceptable as IR and UV fixed point for s_3 but only as UV for s_2. Since UV fixed points are unstable and small corrections push the evolution towards the IR ones, we conclude that the pattern $A_{31} \approx A_{32}$, $|A_{31}| \gg 1$ is unacceptable in the regime in which the approach to the fixed points is relevant.

The remaining degenerate mass patterns can be classified according to the relations $A_{32} \approx A_{21} \approx 0$ or $A_{31} \approx A_{21} \approx 0$. Consider first $A_{21} \approx A_{32} \approx 0$. The equations governing the evolution of the mixing angles can be approximated as

$$\begin{aligned}
\dot{s}_1 &= -s_1 c_1 c_2 s_3 (s_1 s_2 - c_1 c_2 s_3) A_{31} h_\tau^2, \\
\dot{s}_2 &= s_1 c_2^2 (s_1 s_2 - c_1 c_2 s_3) A_{31} h_\tau^2, \\
\dot{s}_3 &= -c_1 c_2 c_3^2 (s_1 s_2 - c_1 c_2 s_3) A_{31} h_\tau^2.
\end{aligned} \tag{33}$$

These equations exhibit IR quasi-fixed point behaviour for $A_{31} < 0$ corresponding to $U_{31} = 0$. As before, at the fixed point the angles satisfy the relation $s_3 = \tan\theta_1 \tan\theta_2$. We recall that this relation is consistent with present experimental information. Since $\dot{s}_1$ is proportional to s_1

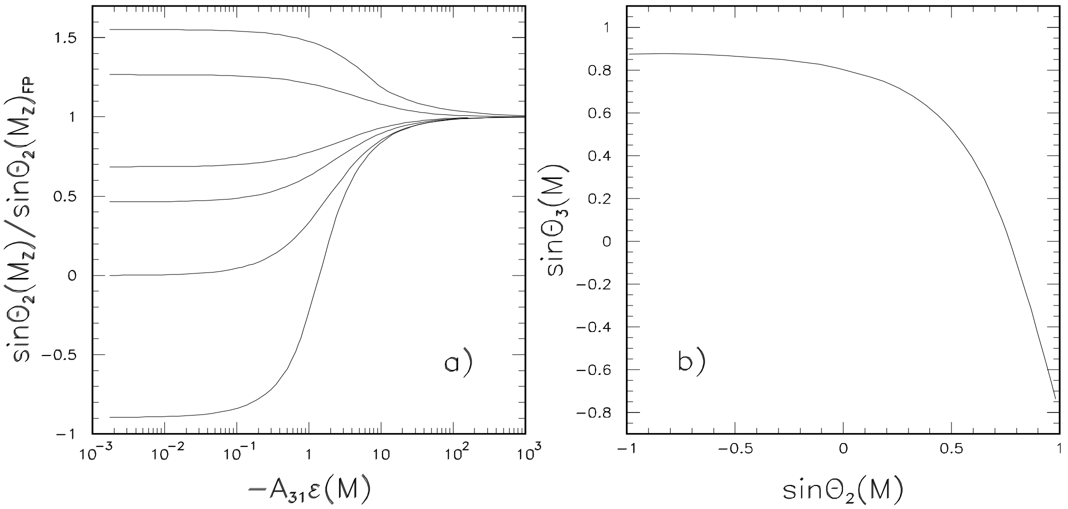

Figure 2: **a)** Approach to the IR fixed point for the degenerate mass pattern $|m_2| \approx |m_1| > |m_3|$ and $m_1 > 0$, $m_2 < 0$, as a function of $-A_{31}\epsilon(M)$ for initial values of $s_2(M)$, $s_3(M)$ and the masses such that $\Delta m^2(M_Z) = 5 \times 10^{-5}$ eV^2, $\Delta M^2(M_Z) = 10^{-3}$ eV^2, $s_3^2(M_Z) = 0.2$ and $\sin^2 2\theta_1(M_Z) = 0.85$ (LAMSW); at the fixed point $\sin^2 2\theta_2(M_Z) = 0.9$. Different lines correspond to different choices of $\theta_2(M)$ **b)** Correlation of $s_2(M)$ and $s_3(M)$ which give experimentally acceptable angles at the fixed point. Parameters at M_Z are as in panel a).

and suppressed by s_3, the running of s_1 is weak. The IR fixed point is reached due to strong running of s_2 and s_3. The rate of approaching the IR fixed point by s_2 is illustrated in Fig. 2a. For $A_{31}\epsilon \gg 1$, $s_2(M_Z)$ is strongly focused at ± 1. Thus, mass and $\tan\beta$ configurations leading to $A_{31}\epsilon \gg 1$ are unacceptable. For $A_{32} < 0$ we get IR fixed point in $U_{32} = 0$.

In summary, with all $|A_{ab}| \lesssim 1$ the evolution of the mixings is negligible. For $|A_{21}| \gg 1$ and $|A_{31}|$, $|A_{32}| \lesssim 1$, or for $A_{32}(A_{31}) \ll -1$ and $A_{31}(A_{32}) \approx A_{21} \approx 0$ the infrared fixed points are reached during the evolution, independently of further details of the mass matrices. We also note that for $|A_{21}| \gg 1$ only s_1 runs to assure the fixed point relation, so already the initial values for s_2 and s_3 at the scale M have to be close to their experimental values. For $A_{31} \ll -1$ or $A_{32} \ll -1$, s_2 and s_3 evolve strongly and the evolution of s_1 is weak. To assure consistency with experimental data, the initial value of s_1 has to be close to the experimental value and the initial values of the other two angles have to satisfy certain relation (see Fig. 2b). Special examples of the IR fixed point behaviour are the textures with exact degeneracy of some masses, which assure the IR fixed point relations already at the scale M. They will be recalled in the last part of the paper.

4 Evolution of mass eigenvalues

The guiding principle for understanding the effects of evolution of mass eigenvalues is eq. (23) and the evolution of the angles. It follows from eq. (23) that quantum corrections $|\Delta m_{ab}^2(M_Z) - \Delta m_{ab}^2(M)|$ are limited from above by $\mathcal{O}(m_{a(b)}^2\epsilon)$ where $\epsilon \approx \tan^2\beta \times 10^{-5}$. In fact, generically this upper bound is saturated (in the sense of order of magnitude) for those mass patterns which give fixed point solutions for mixing angles (at all scales or reachable after the evolution) since then in general $\langle U_{31}^2\rangle \neq \langle U_{32}^2\rangle$ (where $\langle\ldots\rangle$ means average over the evolution). Quantum corrections orders of magnitude smaller than this upper bound can be naturally guaranteed only for weakly evolving angles and with $U_{31}^2 \approx U_{32}^2$. Those two rules determine the order of magnitude of quantum corrections to any mass pattern of interest. We illustrate them with several examples.

The fully hierarchical pattern, with $\Delta M^2 \approx m_3^2 \gg |\Delta m^2| \approx m_{1(2)}^2 \gg m_{2(1)}^2$, is obviously not altered by quantum corrections. Similar conclusion holds for $m_1^2 \approx m_2^2 \sim \mathcal{O}(\Delta m^2)$. More interesting effects may appear for the hierarchy $\Delta M^2 \approx m_3^2 \gg m_1^2, m_2^2 \gg \Delta m^2$ which is possible for the VO solution. It is then interesting to ask the same question which is usually asked [25, 37, 38, 24, 31] for the inversely hierarchical and degenerate patterns: is the initial condition $m_1 = \pm m_2$ at the scale M compatible with the measured (at the scale M_Z) Δm^2 ? We consider first $m_1 = m_2$ which places us in the structure *b*) considered previously for the evolution of the angles. We note that eq. (18) imposes (for $h_\mu = h_e = 0$) at the scale M the fixed point values $U_{31} = 0$ or $U_{32} = 0$. It follows then from the evolution of the masses, eq. (22) and our discussion of the fixed point solutions, that both choices are IR fixed points, so remain stable during the evolution. For $U_{31(32)} = 0$ we get $\Delta m_{21}^2(M_Z) = \pm m_{1(2)}^2(M) 4\epsilon U_{32(31)}^2$, where $U_{32(31)}^2 \sim \mathcal{O}(s_2^2)$. So, for $m_1^2 = m_2^2 \sim 10^{-(6-8)}$ eV and $\tan\beta \lesssim 2.5$ one obtains the right order of magnitude for the VO solution [25].

Choosing $m_1 = -m_2$, the angles remain uncorrelated with the masses (structure *a*)) and stable. For $m_{1(2)}^2 \sim 10^{-(5-8)}$ eV^2 it is easy to choose angles so that $\Delta m_2^2(M_Z) \sim \mathcal{O}(\epsilon m_{1(2)}^2) \sim 10^{-10}$ eV^2 in a large range of $\tan\beta$ values.

One should also note that for the hierarchy I with $m_1^2(M) = m_2^2(M)$ getting the right Δm^2 for SAMSW or LAMSW solutions is only marginally possible for $m_1^2 \gtrsim 10^{-4}$ eV^2 and large values of $\tan\beta$ (> 50).

We consider now the inverse hierarchy $\Delta M^2 \sim m_1^2 \approx m_2^2 \gg m_3^2$. For $m_1(M) = m_2(M)$ we can repeat the previous discussion remembering, however, that now $m_{1(2)}^2 \sim 10^{-3}$ eV^2. Thus, with such initial conditions we cannot reproduce Δm^2 of the VO solution but we naturally get Δm^2 of the SAMSW (for $2.5 \lesssim \tan\beta \lesssim 25$) or LAMSW (for $5 \lesssim \tan\beta$) solutions [25]. And, of course, the mixing angles satisfy one of the fixed point relations for all scales. Note, however, that as stressed earlier the exact degeneracy at M is not necessary to reach the IR fixed point at M_Z

The choice $m_1 = -m_2$ guarantees mild evolution of the elements U_{3a}, $U_{3a}(t) = U_{3a}(0) + \mathcal{O}(\epsilon)$. Since $m_1^2 \approx m_2^2 \sim 10^{-3}$ eV^2 and $\Delta m_{21}^2(M_Z) \lesssim \mathcal{O}(\epsilon m_{1(2)}^2(M))$ we note that choosing the angles in agreement with experimental information we can reproduce the right order of magnitude for Δm^2 for the LAMSW or SAMSW solutions (for roughly the same ranges of $\tan\beta$ as for $m_1 = m_2$). On the other hand, for the VO solution, one needs $\Delta m^2_{21}(M_Z) \approx \mathcal{O}(\epsilon^2 m^2_{1(2)}(M))$ [24]. The absence of $\mathcal{O}(\epsilon m^2_{1(2)}(M))$ contribution to Δm^2 requires $U^2_{31} = U^2_{32}$ which has two solutions:

$$s_3 = -\left(\frac{s_2}{c_2}\right)\frac{c_1 - s_1}{c_1 + s_1} \equiv \frac{s_2}{c_2}\tan\left(\theta_1 - \frac{\pi}{4}\right) \quad \text{or} \tag{34}$$

$$s_3 = \left(\frac{s_2}{c_2}\right)\frac{c_1 + s_1}{c_1 - s_1} \equiv -\frac{s_2}{c_2}\cot\left(\theta_1 - \frac{\pi}{4}\right) \tag{35}$$

independently of $\tan\beta$.

The easiest way to find consistently the mass splitting in order ϵ^2 is to solve the coupled equations (16,19-21) in order ϵ^2 by using the so-called Banach's principle i.e. by substituting in the RHSs of the RGEs their solutions obtained in the order ϵ and integrating once more. One then gets (for definiteness we assume (34) and following ref. [24] take the neutrino mass spectrum in the form $\sim (-1, 1, z)$):

$$\begin{aligned} m_1^2 &= m_\nu^2\left(1 - 4U^2_{31}\epsilon + 8U^4_{31}\epsilon^2 - 4U^2_{31}c_2^2c_3^2\frac{z-1}{z+1}\epsilon^2\right), \\ m_2^2 &= m_\nu^2\left(1 - 4U^2_{31}\epsilon + 8U^4_{31}\epsilon^2 - 4U^2_{31}c_2^2c_3^2\frac{z+1}{z-1}\epsilon^2\right). \end{aligned} \tag{36}$$

where $U^2_{31} = U^2_{32} = (s_2/(s_1 + c_1))^2$. We have used the approximation of constant h_τ and absorbed the overall renormalization introduced by the factor K in eq. (16) in m_ν. We obtain, therefore

$$\Delta m^2 = -16 m_\nu^2 s_2^2 c_2^2 \left(\frac{c_3}{c_1 + s_1}\right)^2 \frac{z}{z^2 - 1}\epsilon^2 \tag{37}$$

For $s_3 = 0$ and $s_1^2 = c_1^2 = 1/2$ this coincides with the result derived in ref. [24]. Since $\Delta M^2 = m^2(z^2 - 1) + \mathcal{O}(\epsilon)$ we get [24]

$$\Delta m^2 = -16\left(\frac{m_\nu^4}{\Delta M^2}\right) s_2^2 c_2^2 \left(\frac{c_3}{c_1 + s_1}\right)^2 z\epsilon^2 \tag{38}$$

We note that for inversely hierarchical pattern, $z = 0$, $\mathcal{O}(\epsilon^2)$ contribution to Δm^2 vanishes too. For $z \sim \mathcal{O}(1)$ the above considerations are applicable also to the degenerate pattern III provided $|A_{31(2)}|\epsilon \lesssim 1$ (see Fig. 2a). With $\epsilon < 2.5 \times 10^{-2}$ for $\tan\beta < 50$ we get $A_{31(2)} < 50$ and $z < 49/51$. For a large range of parameters it is easy to obtain Δm^2 consistent with the VO solution. For the degenerate pattern III with $A_{31(2)}\epsilon \ll -1$ the expansion in ϵ (in fact for the mixing angles this is an expansion in ϵA_{32}) breaks down and this mechanism cannot work.

In general, with the degenerate pattern III, the potentially relevant simple textures are

$$m_3 > |m_1| = |m_2| \qquad \text{or} \qquad |m_1| = |m_2| > m_3.$$

The exact degeneracy of absolute values $|m_3| = |m_2| = |m_1|$ would not result in two distinctly different ΔM^2 and Δm^2 after evolution. With m_1 and m_2 both negative we are in the IR fixed points and encounter similar situation as for the inversely hierarchical case with $m_1 = m_2$. The result $\Delta m^2_{21}(M_Z) \sim \mathcal{O}(\epsilon m^2_{1(2)}(M))$ is compatible with the LAMSW and SAMSW solutions but not with the VO solution. However, the relation $\Delta m^2_{31}(M_Z) \sim \Delta m^2_{32}(M_Z) \approx \Delta M^2$ can be simultaneously satisfied only if all masses squared are of order $\Delta M^2 \sim 10^{-(3-2)}$ and therefore we need $2.5 \lesssim \tan\beta \lesssim 15$ ($5 \lesssim \tan\beta$) for the SAMSW (LAMSW) solution. As explained in the previous section, both masses positive are unacceptable in the regime in which the fixed points are relevant.

For $m_1 = -m_2$ we get $A_{21} = 0$, $A_{32} \approx 0$ for positive m_1 and $A_{21} = 0$, $A_{31} \approx 0$ for negative m_1, with $|A_{31}| \gg 1$ and $|A_{32}| \gg 1$, respectively. Such initial conditions assure the reaching of IR fixed points at $U_{31} = 0$ for $A_{31}\epsilon \ll -1$ or $U_{32} = 0$ for $A_{32}\epsilon \ll -1$ and, from the point of view of quantum corrections to the masses, we are back to the same situation as for m_1 and m_2 both negative. For $|A_{31(2)}|\epsilon \lesssim 1$ but $A_{31(2)} \ll -1$ the angles evolve very mildly and the previously described mechanism of stabilization can assure right Δm^2 for the VO solution

5 Conclusions

In this paper we have derived RG equations directly for the mixing angles and mass eigenvalues. These equations allow for easy qualitative discussion of the evolution of masses and mixing angles, which systematizes existing results [31, 25, 24, 37, 38, 26] and allows for their generalization. The equations for the mixing angles have IR fixed points at $U_{31} = 0$ or $U_{32} = 0$, which are reachable for several mass hierarchies consistent with the measured mass squared differences and characterized by one large factor $|A_{ab}| \equiv |(m_a + m_b)/(m_a - m_b)| \gg 1$ with all other $|A_{ab}|$'s $\lesssim \mathcal{O}(1)$. Both fixed points give relation (32) which is at present acceptable experimentally. Its further verification, by clarifying the LSND puzzle, measuring s_3 and discriminating between large and small solar angle solutions is of obvious interest.

Special examples of the IR fixed points behaviour are the textures with exact degeneracy of some masses. The mass squared differences consistent with the measured values can be obtained for the following textures: *i)* hierarchical with $|m_3| \sim 10^{-1.5}$ eV, $m_1 = m_2$ and $|m_1| \sim 10^{-(3-4)}$ eV (for VO), *ii)* inversely hierarchical with $m_1 = m_2 \sim 10^{-1.5}$ eV $\gg m_3$ (for LAMSW and SAMSW), *iii)* degenerate with $|m_i| \gtrsim \mathcal{O}(0.1)$ eV ($i = 1, 2, 3$) and $m_1 = m_2 < 0$ or $m_1 = -m_2$ with $A_{31}\epsilon \ll -1$ (for LAMSW and SAMSW).

With the fully hierarchical masses $|m_3| \sim 10^{-1.5}$ eV, $m_2^2 \sim \Delta m^2 \gg m_1^2$ and for the inverse hierarchy with $m_1 = -m_2$ the evolution of the angles is very mild. The proper order of magnitude for Δm^2 is possible for the LAMSW and SAMSW solutions. Similarly mild evolution occurs for the degenerate case with $m_1 = -m_2$, $|A_{31(2)}|\epsilon \lesssim 1$, $A_{31(2)} \ll -1$ which is consistent with the stabilization mechanism leading to Δm^2 of the VO solution.

We focused our discussion on the MSSM. The corresponding RG equation in the SM are obtainable by the replacements mentioned in the text. The UV and IR fixed points are interchanged and the running of the angles is weaker by factor 2 than for $\tan\beta = 1$ in the MSSM.

Acknowledgments

The work of P.H.Ch. was partly supported by the Polish State Committee for Scientific Research grant 2 P03B 030 14 (for 1998–1999) and by the Maria-Skłodowska-Curie Joint Fund II (MEN/DOE-96-264). The work of W.K. and S.P. was partly supported by the Polish State Committee for Scientific Research grant 2 P03B 052 16 (for 1999–2000). P.Ch. and S.P. would like to thank Santa Cruz Institute for Particle Physics and Institute de Physique Nucleaire in Lyon, respectively, for warm hospitality during the completion of this work. S.P. is indebted to Stavros Katsanevas for interesting discussions on neutrino physics

References

[1] Y. Fukuda et al., Superkamiokande Collaboration, *Phys. Lett.* **B433** (1998) 9, *Phys. Rev. Lett.* **81** (1998) 1562; S. Hatakeyama et al., Kamiokande Collaboration, *Phys. Rev. Lett.* **81** (1998) 2016.

[2] B.T. Cleveland et al., *Astrophys. J.* **496** (1998) 505; K.S. Hirata et al., Kamiokande Collaboration, *Phys. Rev. Lett.* **77** (1996) 1683; W. Hampel et al., GALLEX Collaboration, *Phys. Lett.* **B388** (1996) 384; D.N. Abdurashitov et al., SAGE Collaboration, *Phys. Rev. Lett.* **77** (1996) 4708; Y. Suzuki, talk at the conference *Neutrinos'98* Takayama, Japan, June 1998.

[3] A. Apollonio et al., CHOOZ Collaboration, *Phys. Lett.* **B420** (1998) 397.

[4] B. Achkar et. al., LSND Collaboration *Nucl. Phys.* **B434** (1995) 503, D.H. White, talk at the conference *Neutrinos'98* Takayama, Japan, June 1998.

[5] W. Królikowski preprints IFT-99/08 (hep-ph/9904489) and IFT-99/24 (hep-ph/9910308).

[6] Z. Maki, M. Nakagawa and S. Sakata, *Prog. Theor. Phys.* **28** (1962) 870.

[7] S.M. Bilenkii, C. Giunti and W. Grimus, preprint UWTHPH-1998-61 (hep-ph/9812360); S.T. Petcov, talk on 17^{th} *Int. Workshop on Weak Interactions and Neutrinos*, Cape Town, South Africa, January 1999.

[8] R. Barbieri et al., *JHEP* (1998) 9812:017.

[9] G.L. Fogli, E. Lisi, A. Marrone and G. Scioscia, *Phys. Rev.* **D59** (1999) 033001.

[10] J.S. Kim and C.W. Kim, hep-ph/9909428

[11] S. Dimopoulos, L.J. Hall and S. Raby, *Phys. Rev.* **D47** (1993) 3697.

[12] T. Blazek, S. Raby and K. Tobe, preprint OHSTPY-HEP-T-98-030 (hep-ph/9903340).

[13] G.K. Leontaris, S.Lola and G.G. Ross, *Nucl. Phys.* **B454** (1995) 25.

[14] G.K. Leontaris, S. Lola, C. Scheich, *Phys. Rev.* **D53** (1996) 6381.

[15] S. Lola, J.D. Vergados, *Prog. Part. Nucl. Phys.* **40** (1998) 71.

[16] R. Barbieri, L.J. Hall, A. Strumia, *Phys. Lett.* **B445** (1999) 407.

[17] G. Altarelli and F. Feruglio, *Phys. Lett.* **B439** (1998) 112, *JHEP* **9811:021** (1998), *Phys. Lett.* **B451** (1998) 388, preprint CERN-TH-99-129 (hep-ph/9905536), to appear in proceedings of *8th International Workshop on Neutrino Telescopes*, Venice, Italy, Feb 1999; G. Altarelli, F. Feruglio and I. Masina, preprint CERN-TH-99-147 (hep-ph/9907532).

[18] S. Lola and G.G. Ross, *Nucl. Phys.* **B553** (1999) 81.

[19] R. Barbieri, L.J. Hall, G.L. Kane and G.G. Ross, preprint OUTP-9901-P (hep-ph/9901228).

[20] M. Jeżabek and Y. Sumino, *Phys. Lett.* **B440** (1998) 327, *Phys. Lett.* **B457** (1999) 139.

[21] M. Carena, J. Ellis, S. Lola and C.E.M. Wagner, preprint CERN-TH-99-173 (hep-ph/9906362).

[22] B. Stech, preprint HD-THEP-99-15 (hep-ph/9905440).

[23] M. Olechowski and S. Pokorski, *Phys. Lett.* **B257** 1991, 388.

[24] R. Barbieri, G.G. Ross and A. Strumia, preprint OUTP-99-30-P (hep-ph/9906470).

[25] J.A. Casas, J.R. Espinosa, A. Ibarra and I. Navarro, *JHEP* 9909:015 (1999).

[26] N. Haba, N. Okamura and M. Sugiura, preprint KEK-TH-597 (hep-ph/9810471); N. Haba, Y. Matsui, N. Okamura and M. Sugiura, preprint KEK-TH-620 (hep-ph/9904292); N. Haba and N. Okamura, preprint KEK-TH-632 (hep-ph/9906481).

[27] C. Wetterich, *Nucl. Phys.* **B187** (1981) 343.

[28] P.H. Chankowski and Z. Płuciennik, *Phys. Lett.* **B316** (1993) 312.

[29] P.H. Chankowski, *Phys. Rev.* **D41** (1990) 2877.

[30] K. Babu, C.N. Leung and J. Pantaleone, *Phys. Lett.* **B319** (1993) 191.

[31] J. Ellis and S. Lola, *Phys. Lett.* **B458** (1999) 310.

[32] K. Babu, *Z. Phys.* **C35** (1987) 69.

[33] M. Tanimoto, *Phys. Lett.* **B360** (1995) 41.

[34] J. Ellis, G.K. Leontaris, S. Lola and D.V. Nanopoulos, *Eur. Phys. J.* **C9** (1999) 389-408.

[35] S. Lola, preprint CERN-TH-99-40, to appear in the proceedings of the 6th Hellenic School and Workshop on Elementary Particle Physics, Corfu, Greece, Sep 1998 (hep-ph/9903203).

[36] E. Ma, preprint UCRHEP-T259 (hep-ph/9907400)

[37] J.A. Casas, J.R. Espinosa, A. Ibarra and I. Navarro, *Nucl. Phys.* **B556** (1999) 3.

[38] J.A. Casas, J.R. Espinosa, A. Ibarra and I. Navarro, preprint CERN-TH/99-142 (hep-ph/9905381).